SECTION 16

ANTENNAS AND WAVE PROPAGATION

An antenna can be thought of as the control unit between a source and some medium that will propagate an electromagnetic wave. In the case of a wire antenna, it can be seen as a natural extension of the two-wire transmission line, and, in a similar way, a horn antenna can be considered a natural extension of the waveguide that feeds the horn.

The radiation properties of antennas are covered in Chap. 16.1. They include gain and directivity, beam efficiency, and radiation impedance. Depending on the antenna application, certain parameters may be more important. For example, in the case of receiving antennas that measure noise signals from an extended source, beam efficiency is an important measure of its performance.

Chapter 16.2 examines the various types of antennas, including simple wire antennas, waveguide antennas useful in aircraft and spacecraft applications, and low-profile microstrip antennas.

Finally, Chap. 16.3 treats the propagation of electromagnetic waves through or along the surface of the earth, through the atmosphere, and by reflection or scattering from the ionosphere or troposphere. More details of propagation over the earth through the nonionized atmosphere and propagation via the ionosphere are covered on the accompanying CD-ROM. D.C.

In This Section:

On the CD-ROM:

Kirby, R. C., and K. A. Hughes, *Propagation over the Earth Through the Nonionized Atmosphere*, reproduced from the 4th edition of this handbook.

Kirby, R. C., and K. A. Hughes, *Propagation via the Ionosphere*, reproduced from the 4th edition of this handbook.

CHAPTER 16.1
PROPERTIES OF ANTENNAS AND ARRAYS

William F. Croswell

ANTENNA PRINCIPLES

The radiation properties of antennas can be obtained from source currents or fields distributed along a line or about an area or volume, depending on the antenna type. The magnetic field ***H*** can be determined from the vector potential as

$$\mathbf{H} = \frac{1}{\mu} \nabla \times \mathbf{A} \tag{1}$$

To determine the form of **A** first consider an infinitesimal dipole of length L and current I aligned with the z axis and placed at the center of the coordinate system given in Fig. 16.1.1.

$$A = z[\mu IL \exp(-jkr)]/4\pi r \tag{2}$$

where $k = 2\pi/\lambda$, and r is the radial distance away from origin in Fig. 16.1.1. From Eqs. (1) and (2) and Maxwell's equations, the fields of a short current element are

$$\begin{aligned} H_\phi &= \frac{jkIL \sin\theta}{4\pi r}\left(1+\frac{1}{jkr}\right)\exp(-jkr) \\ E_\theta &= \frac{jkLI\eta \sin\theta}{4\pi r}\left(1+\frac{1}{jkr}-\frac{1}{k^2r^2}\right)\exp(-jkr) \\ E_r &= \frac{IL\eta}{2\pi r}\cos\theta\left(1+\frac{1}{jkr}\right)\exp(-jkr) \end{aligned} \tag{3}$$

when $\eta = \sqrt{\mu/\epsilon}$ and ϵ = permitivity of source medium.

By superposition, these results can be generalized to the vector of an arbitrary oriented volume-current density **J** given by

$$A(x, y, z) = \frac{\mu}{4\pi}\int_{r'} \mathrm{J}(x', y', z')\frac{\exp(-jkR)}{R}dx'\,dy'\,dz' \tag{4}$$

For a surface current, the volume-current integral Eq. (4) reduces to a surface integral of $\mathbf{J}_s[\exp(-jkR)]/R$, and for a line current reduces to a line integral of **I** $[\exp(-jkR)]/R$. The fields of all physical antennas can be

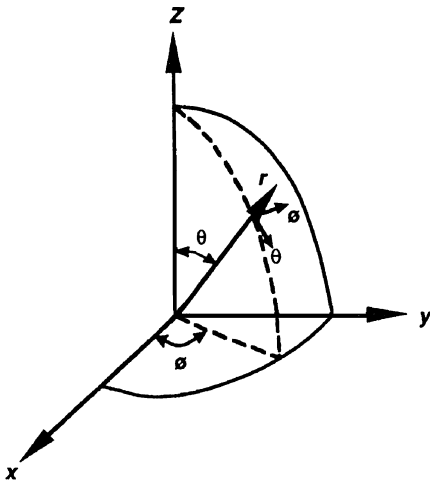

FIGURE 16.1.1 Spherical coordinate system with unit vectors.

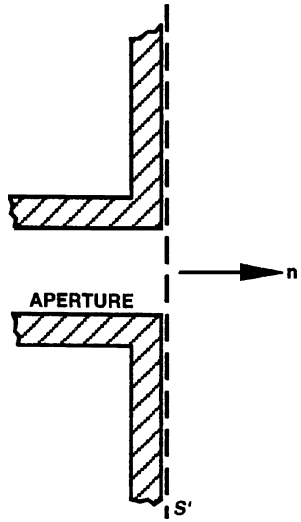

FIGURE 16.1.2 Equivalent aperture plane for far-field calculations: $\mathbf{M} = 2\mathbf{E}_s \times \hat{\mathbf{n}}$. $\mathbf{J} = 2\hat{\mathbf{n}} \times \mathbf{H}'_s$, and $\mathbf{J} = \mathbf{n} \times \mathbf{H}'_s$, $\mathbf{M} = \mathbf{E}'_s \times \hat{\mathbf{n}}$.

obtained from the knowledge of **J** alone. However, in the synthesis of antenna fields the concept of a magnetic volume current **M** is useful, even though the magnetic current is physically unrealizable. In a homogeneous medium the electric field can be determined by

$$\mathbf{E} = \frac{1}{\epsilon}\nabla \times \mathbf{F} \qquad F = \frac{\epsilon}{4\pi}\int_{r'} M(x',\, y',\, z')\frac{\exp\,(-jkR)}{R}dx'\,dy'\,dz' \tag{5}$$

Examples of antennas that have a dual property are the thin dipole in free space and the thin slot in an infinite ground plane. The fields of an electric source **J** can be determined using Eqs. (1) and (5) and Maxwell's equations. From the far-field conditions and the relationships between the unit vectors in the rectangular and spherical coordinate systems, the far fields of an electric source **J** are

$$\begin{aligned}\eta H_\theta^J = {} & \frac{-jnk\exp(-jkr)}{4\pi r}\int_v (J_{x'}\cos\theta\,\cos\phi \\ & + J_{y'}\cos\theta\,\sin\phi - J_{z'}\sin\theta)\exp[jk(x'\sin\theta\cos\phi \\ & + y'\sin\theta\,\sin\phi + z'\cos\theta)]\,dx'\,dy'\,dz'\end{aligned} \tag{6}$$

$$\begin{aligned}-\eta H_\theta^J = E_\phi^J = {} & \frac{j\eta k\exp(-jkr)}{4\eta r}\int_{v'} (J_{x'}\sin\phi \\ & - J'_y\cos\phi)\exp[\,jk(x'\sin\theta\cos\phi \\ & + y'\sin\theta\,\sin\phi\, + z'\cos\theta]\,dx'\,dy'\,dz'\end{aligned} \tag{7}$$

In a similar manner the radiated far fields from a magnetic current **M** are

$$\begin{aligned}\eta H_\phi^M = E_\theta^M = {} & \frac{-jk\exp(-jkr)}{4\pi r}\int_{v'} (M_{y'}\cos\phi \\ & - M_{x'}\sin\phi)\,\exp[jk(x'\sin\theta\cos\phi \\ & + y'\sin\theta\,\sin\phi\, + z'\cos\theta]\,dx'\,dy'\,dz'\end{aligned} \tag{8}$$

$$\eta H_\theta^M = E_\phi^M = \frac{-jk\ \exp(-jkr)}{4\pi r}\int_{v'}(M_{x'}\cos\phi\cos\theta + M_{y'}\sin\phi\cos\theta - M_{z'}\sin\theta)\exp[jk(x'\sin\theta\cos\phi + y'\sin\theta\sin\phi + z\cos\theta]\ dx'\,dy'\,dz' \tag{9}$$

Currents and Fields in an Aperture

For aperture antennas such as horns, slots, waveguides, and reflector antennas, it is sometimes more convenient or analytically simpler to calculate patterns by integrating the currents or fields over a fictitious plane parallel to the physical aperture than to integrate the source currents. Obviously, the fictitious plane can be chosen to be arbitrarily close to the aperture plane. If the integration is chosen to be an infinitesimal distance away from the aperture plane, the fields to the right of s' in Fig. 16.1.2 can be found using either of the equivalent currents

$$\mathbf{M}_{s'} = 2\mathbf{E}_{s'} \times \hat{\mathbf{n}} \tag{10a}$$

$$\mathbf{J}_{s'} = 2\hat{\mathbf{n}} \times \mathbf{H}_{s'} \tag{10b}$$

$$\mathbf{J}_{s'} = \hat{\mathbf{n}} \times \mathbf{H}_{s'} \quad \text{and} \quad \mathbf{M}_{s'} = -\hat{\mathbf{n}} \times \mathbf{E}_{s'} \tag{10c}$$

The combined electric and magnetic current given in Eq. (10*c*) is the general Huygens' source and is generally useful for aperture problems where the electric and magnetic fields are small outside the aperture: In limited cases, the waveguide without a ground plane, a small horn, and a large tapered aperture can be approximated this way.

Far Fields of Particular Antennas

From the field equations stated previously or coordinate transformations of these equations, the far-field pattern of antennas can be determined when the near-field or source currents are known. Approximate forms of these fields or currents can often be estimated, giving good pattern predictions for practical purposes.

Electric Line Source

Consider an electric line source (current filament) of length L centered on the z' axis of Fig. 16.1.1 with a time harmonic-current $I(z')e^{j\omega t}$. The fields of this antenna are, from Eq. (6),

$$E_\theta = \frac{jnk\ \sin\theta\ \exp(-jkr)}{4\pi r}\int_{-L/2}^{L/2} I(z')\ \exp[-jkz'\ \cos\theta)]dz'\ \ E_\phi = 0$$

For the short dipole where $kL \ll 1$ and $I(z') = I_0$

$$E_\theta = [j\eta kLI_0\ \exp(-jkr)\ \sin\theta]/4\pi r$$

which agrees with Eq. (3).

Electric Current Loop

The far fields of an electric current loop of radius a, centered in the xy plane of Fig. 16.1.1, which has a current flowing on it can be obtained by returning to the vector potential $\mathbf{A}$ and deriving the expressions similar to Eqs. (6) and (7) using a potential $A_\phi = A_\tau$. The resulting field is

$$E\theta = \frac{-j\eta \exp(-jkr)\cos\theta}{4\pi r}\int_0^{2\pi} I(\phi')\sin(\phi-\phi')\exp[jka\cos(\phi-\phi^1)\sin\theta]d\phi'$$

$$E_\phi = \frac{-jk \exp(-jkr)\cos\theta}{4\pi r}\int_0^{2\pi} I(\phi')\cos(\phi-\phi')\exp[jka\cos(\phi-\phi')\sin\theta]d\phi'$$

The fields for the constant current loop. $I(z') = I_0$ with a radius $a << \lambda$, are

$$E\phi = (k^2a^2\eta/r)I_0 \exp(-jkr)\sin\theta$$

Note that $E_\theta = 0$. The field of the small loop is similar to the field produced by a constant magnetic current source of length L, where $L << \lambda$.

Elementary Huygens' Source

Assume that constant electric and magnetic current sources $J_{x'} = J_0$ and $M_{y'} = M_0$ of equal length $L << \lambda$ are simultaneously placed at the origin of Fig. 16.1.1. If the currents are adjusted such that $\eta J_0 L = M_0 L$, the far fields of this source are

$$E_\theta = \frac{-jk\exp(-jkr)}{4\pi r}\cos\phi(1+\cos\theta)J_0L$$

$$E\phi = \frac{jk\exp(-jkr)}{4\pi r}\sin\phi(1+\cos\theta)J_0L$$

The unique feature of this fictitious source compared with the electric or magnetic current element alone is the obliquity factor $(1 + \cos\theta)$, which tends to cancel the far-field radiation pattern in the region $\pi/2 \le \theta \le \pi$ due to its cardioid shape. Aperture antennas have field distributions which can be constructed from Huygens' source elements having the patterns described above.

Aperture in Infinite Ground Plane

With the equivalent current $\mathbf{M}_{s'} = -2\mathbf{z} \times \mathbf{E}_{s'}$, the far field of a waveguide aperture opening onto an infinite ground plane can be obtained by integrating the aperture field since the tangential electric field is zero on the ground plane. From the magnetic current and Eqs. (6) to (9), the far-field patterns of the dominant-mode circular and rectangular waveguides can be derived.

Simple Arrays

Consider a linear array of radiating elements which, for simplicity, are assumed to be equally spaced at a distance d apart, as illustrated in Fig. 16.1.3. The field at a large distance away from the mth element can be written

$$E_m = f_m(\theta, \phi)\frac{\exp(-jkr)}{r}\exp(jk_m d\cos\theta) \tag{11}$$

By superposition the field of an array of N elements is given by

$$E_N = \frac{-\exp(-jkr)}{r}\sum_{m=1}^{N} f_m(\theta, \phi)\exp[-j(m-1)kd\cos\theta] \tag{12}$$

If the element at the origin is chosen as a reference. If each element has an identical pattern, $f_m(\theta, \phi) = a_m E(\theta, \phi)$ and

$$E_n(\theta, \phi) = E(\theta, \phi), f(\varphi)$$
$$f(\varphi) = \sum_{m=1}^{N} a_m \exp j\varphi \tag{13}$$

where a_m is a complex number representing the excitation current (voltage in the case of slots) for the mth element and $\varphi = -(m-1)kd \cos \theta$. The function $f(\varphi)$ is commonly called the *array factor* or *array polynomial*, and the factorization process given in Eq. (13) is called *pattern multiplication*.

Uniform Linear Array

Suppose the array of point sources in Fig. 16.1.3 is fed uniformly in amplitude and has a phase shift δ between adjacent elements. Here $a_m = e^{-jm\delta}$ and $\varphi = kd \cos \theta - \delta$, and consequently $|f(\theta, \phi)|^2$ is as follows:
General:

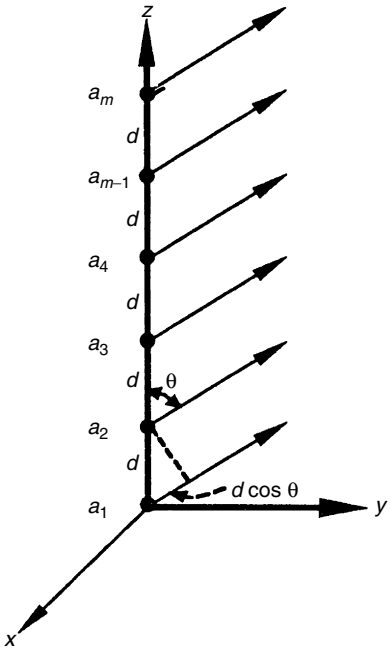

FIGURE 16.1.3 Geometry of a linear array of equally spaced elements.

$$|f(\theta, \phi)|^2 = \left| \frac{\sin^2[(N/2)(kd \cos\theta - \delta)]}{N^2 \sin^2[(kd/2)\cos\theta - \delta]} \right| \tag{14}$$

Broadside $\delta = 0$:

$$|f(\theta, \phi)|^2 = \left| \frac{\sin^2[(N/2)(kd \cos\theta)]}{N^2 \sin^2[(kd/2)\cos\theta]} \right| \tag{15}$$

End fire $\delta = kd$:

$$|f(\theta, \phi)|^2 = \left| \frac{\sin^2[(Nkd/2)(\cos\theta - 1)]}{N^2 \sin^2[kd/2)(\cos\theta - 1)]} \right| \tag{16}$$

Owing to the ϕ rotational symmetry in Eq. (14), the pattern of the line source has rotational symmetry about the z axis. As the cone angle of the pattern decreases with scan angle from broadside, the pattern directivity remains constant at the value N regardless of scan angle. By choosing the phase shift between elements so that $\delta = kd + 2.94/N$ the sharpest pattern in the end-fire direction ($\theta = 0$) is obtained. In this case

$$|f(\theta, \phi)|^2 = \left| \frac{\sin^2[(Nkd/2)(k \cos\theta - k')]}{N^2 \sin^2[(d/2)(k \cos\theta - k')]} \right| \tag{17}$$

where $k' = k + 2.94/Nd$. This phase condition, which is determined graphically, is called the *Hansen-Woodward condition* for superdirectivity. This extra directivity may be several decibels in practical antennas.

Circular Arrays

Consider an array of N equally spaced elements about a circle of radius a in the xy plane of Fig. 16.1.1. If the azimuthal location of the mth element is $\phi_m = 2\pi m/N$, then for an element excitation of the form $a_m = A_{mn}e^{Ja_m}$ the array factor is given by

$$f(\theta, \phi) = \sum_{m=1}^{N} A_m \exp\{j[\alpha_m + ka \sin\theta \cos(\phi - \phi_m)]\} \tag{18}$$

For arrays having a large number of elements, $|A_m|$ = const, the array-factor pattern in the xy plane can be approximated by

$$|f(\theta, \phi = \pi/2)| \approx |\mathbf{J}_0[2ka \sin 1/2(\phi - \phi_0)]|$$

which is a directional beam with a maximum of $\phi = \phi_0$. If the pattern of each antenna in the circular array is of the form $F(\phi) = \Sigma_{m=0}^{\infty} A_m \cos^m \phi$, the pattern of a uniformly excited circular array of N such elements is approximately given by

$$\Phi(\theta, \phi) \approx N \sum_{m=0}^{M} A_m (-i)^m \frac{d^m}{dz^m}[J_0(z) + 2j^N J_m(z) \cos N\phi] \tag{19}$$

where $M < N$ and $Z = ka \sin\theta$. A design curve for determining the number of sources N required in a circular array of circumference Z to produce an omnidirectional pattern with 0.5 dB ripple or less is given in Ref. 1.

Planar Arrays

Now consider a planar array of equally spaced elements in the yz plane of Fig. 16.1.3, where the elements in the y direction are a distance d from the elements on the axis. With the origin as a phase reference, the array factor is given by

$$f(\theta, \phi) = \sum_{n=1}^{N} \sum_{m=1}^{M} a_{mn} \exp[jk(nd \cos\theta + md \sin\theta \sin\phi)] \tag{20}$$

where the excitation coefficient $a_{mn} = A_{mn} \exp[jk(m\delta_y + n\delta_z)]$. If $A_{mn} = 1$ and $\delta_y = \delta_z = 0$, the array has a pattern maximum at broadside and has the array factor

$$|f(\theta, \phi)|^2 = \left| \frac{\sin^2(Nkd/2)\cos\theta}{N^2 \sin[(kd/2)\cos\theta]} \right| \left| \frac{\sin^2(Mkd/2)\cos\theta \sin\phi}{M^2 \sin^2[(kd/2)\cos\theta \sin\phi]} \right| \tag{21}$$

The pattern in the two principal planes of the uniformly excited array is identical in form to the linear array in the same plane. As the array is scanned from broadside, the pattern broadens and becomes asymmetrical.

Gain and Directivity

Antennas that are several wavelengths or larger in dimension have far-field patterns for which most of the radiated energy is restricted to narrow angular regions. Several useful measures of how the pattern is concentrated are gain, directivity, effective area, and beam efficiency. The beam efficiency is important for low-noise

communication systems, microwave radiometry, and radio-astronomy antennas. The definitions of directional directivity $D(\theta, \phi)$, directivity D, gain G, and directional $G(\theta, \phi)$ are:

$$G(\theta, \phi) = N_A(1 - |\Gamma|^2)[D(\theta, \phi)] = N_A(1 - |\Gamma|^2)\left[4\pi \frac{\text{power radiated in direction } (\theta, \phi)}{\text{total power radiated by antenna}}\right]$$

$$G = N_A(1 - |\Gamma|^2)[D = N_A(1 - |\Gamma|^2)\left(4\pi \frac{\text{maximum power radiated by antenna}}{\text{total power radiated by antenna}}\right)$$

The term N_A is the antenna efficiency related to I^2R losses, and Γ is the reflection coefficient as seen at the antenna input terminals. In equation form

$$D(\theta, \phi) = \frac{4\pi |E(\theta, \phi)|^2}{\int_0^{2\pi} \int_0^{\pi} |E(\theta, \phi)|^2 \sin\theta \, d\theta \, d\phi} \tag{22}$$

where $E(\theta, \phi)$ = electric field of the antenna, and

$$D = \frac{4\pi |E(\theta, \phi)|^2 \max}{\int_0^{2\pi} \int_0^{\pi} |E(\theta, \phi)|^2 \sin\theta \, d\theta \, d\phi} \tag{23}$$

An example of the directivity of two-dimensional arrays is given in Fig. 16.1.4. The element pattern is of the form $2J_1(c_\theta)/C_\theta$, which approximates the elements such as slots and dipoles. Other calculations for different element patterns are given in Eqs. (2) and (3).

Beam Efficiency

In addition to the gain of an antenna, the beam efficiency is a very useful parameter for judging the quality of receiving antennas intended for measurement of noise signals from an extended source. The beam efficiency is a measure of the ability of an antenna to discriminate between the received signal in the main beam and unwanted signals received through the side lobes in other directions. Assuming that the antenna aperture is in the xy plane in Fig. 16.1.1, the beam efficiency is defined as

$$BE = \frac{\text{power radiated in a cone angle } \theta_1}{\text{total power radiated by the antenna}} = \frac{\int_0^{2\pi} \int_0^{\theta_1} |E(\theta, \phi)|^2 \sin\theta \, d\theta \, d\phi}{\int_0^{2\pi} \int_0^{\pi} |E(\theta, \phi)|^2 \sin\theta \, d\theta \, d\phi} \tag{24}$$

Beam efficiency varies significantly dependent on the shape of the aperture and the aperture distribution. Calculations for circular apertures with a symmetrical distribution $f(p) = [1 - (p/a)^2]N$ are given in Fig. 16.1.5. This distribution approximates the aperture field of parabolic antennas. Calculations for square apertures with field distribution $f(x) = \cos^n(x/a)$ are given in Fig. 16.1.5. Further beam efficiencies for circular apertures with different field distributions are given in Eqs. (4) and (5).

Antenna Temperature

An antenna located on the earth and pointing at an angle (θ, ϕ) to the sky will receive noise from all directions. The amplitude of this noise as seen at the antenna terminals will depend on the noise source (warm earth, cosmic noise,

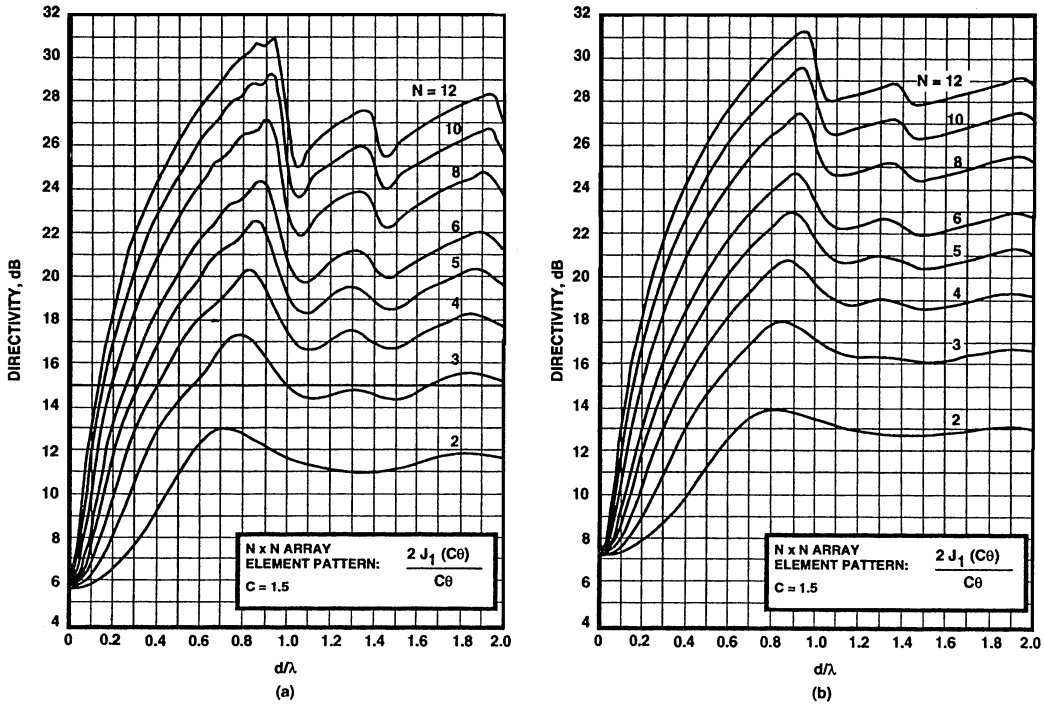

FIGURE 16.1.4 Directivities for uniformly excited $M \times N$ arrays with the element pattern of $2J_1(C_\theta)/C_\theta$ (after Ref. 2): (*a*) $c = 1.5$, (*b*) $c = 2$.

water vapor, radio stars, and so forth), the antenna orientation, and the operating frequency and polarization. The equivalent received noise power in a receive matched to the antenna terminal impedance by a lossless transmission line is

$$P_n = kTB \tag{25}$$

where k = Boltzmann's constant
T = temperature (K)
B = bandwidth (Hz)

Noise power for a fixed bandwidth may be thought of an equivalent temperature. Consequently, if it is assumed that the various noise sources that make up the antenna noise environment have an equivalent temperature $T(\theta, \phi)$ the apparent antenna temperature is given by

$$T_A = \frac{\int_0^{2\pi} \int_0^{\pi} G(\theta, \phi)\, T(\theta, \phi) \sin\theta \, d\theta \, d\phi}{\int_0^{2\pi} \int_0^{\pi} G(\theta, \phi) \sin\theta \, d\theta \, d\phi} \tag{26}$$

The most important natural emitter of noise at microwave frequencies is the ground at 377 K compared with the sky temperature at a few degrees. Therefore, antennas that have low side and back lobes will have low apparent antenna temperatures T_A.

PROPERTIES OF ANTENNAS AND ARRAYS

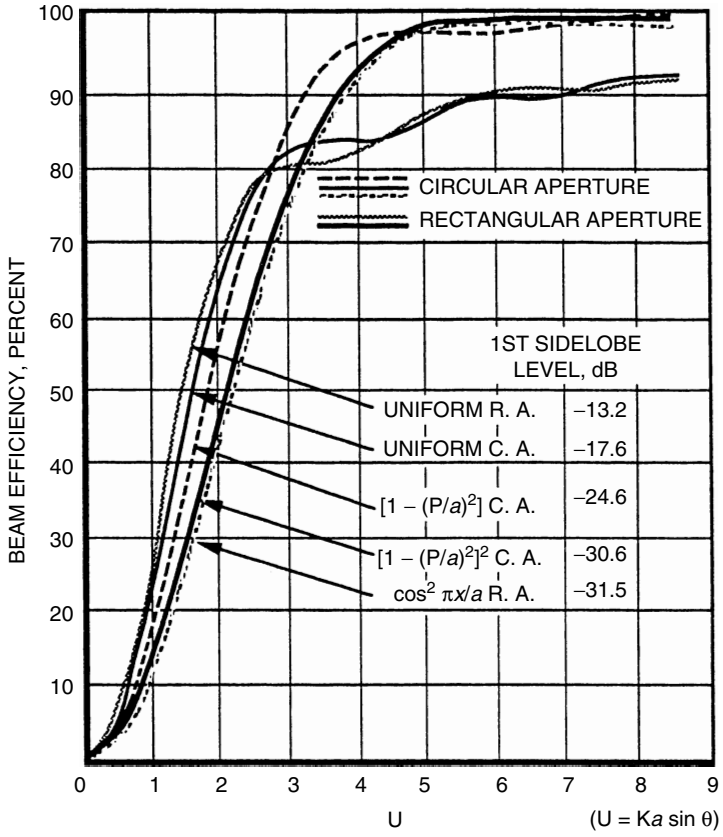

FIGURE 16.1.5 Beam efficiencies of rectangular apertures (RA) and circular apertures (CA) with various aperture distributions.

If the antenna has losses and is not matched to the receiver for maximum power transfer, the antenna temperature will be higher than predicted by Eq. (26). The contribution due to the particular mismatch and losses of every component must be analyzed for each particular receiving system in detail. An outline of an excellent method of analysis is available.[6] For a receiving system with no mismatch loss, the apparent temperature T_a is given by

$$T_a = (1-L)T_A + LT_0 \tag{27}$$

where T_A is the antenna temperature given by Eq. (27) and T_0 is the physical temperature of lossy device.

Friis Transmission Formula

Assume that there is a source antenna and an antenna under test located at a distance r apart such that

$$r \geq 2(d_t)^2/\lambda \tag{28}$$

where d_t is the maximum aperture dimension of the antenna under test. The distance specified by Eq. (28) is the so-called *far-field distance*. The far-field distance is commonly specified as the distance where the phase front of a spherical wave over a planar aperture will not exceed $\pi/8$ rad. For special purposes, such as

the measurement of deep nulls or extremely precise side-lobe levels, the far-field distance may have to be extended further; curves using other criteria are available.[7] The power received at the terminals of one antenna located in the far field of a second antenna can be expressed as a fraction of the transmitted power as

$$P_R = P_T\{\lambda/4\pi r]^2 N_{AT} N_{AR} D_T(\theta_T, \phi_T) D_R(\theta_R, \phi_R)(1-|\Gamma_r|^2)(1-|\Gamma_r|^2)\,|\rho_R \cdot \rho_T|^2 \tag{29}$$

where N_{AT}, N_{AR} are loss efficiencies of antennas and $D_T(\theta_T, \phi_T)$, $D_R(\theta_R, \phi_R)$ are directivities of antennas in the direction one antenna is pointing toward the other. $|\Gamma_T|^2$ and $|\Gamma_R|^2$ are the reflected power due to mismatch of the antenna terminals and $|\rho_R \cdot \rho_T|^2$ is the polarization loss. The term in brackets in Eq. (29) is the so-called free-space loss, which is a result of spherical spreading of the energy radiated by an antenna. In the far field all antennas appear as a spherical wave emanating from a point source located at the phase center of the antenna, where the phase center may be a function of the observation angle.

Polarization

Consider a plane wave propagating in the z direction, which has an arbitrary plane polarization with an axial ratio r_A is defined as the ratio of the major to minor axis of the ellipse referenced to a coordinate system (Fig. 16.1.6). The field expression for this arbitrary plane-polarized wave is

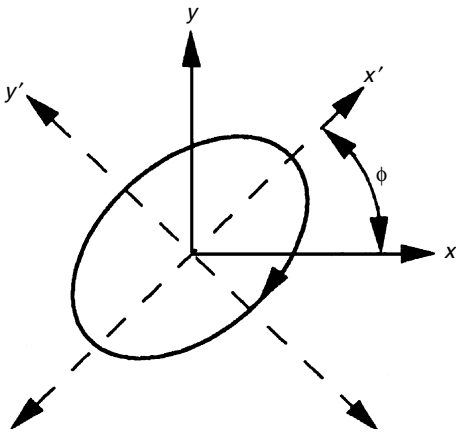

FIGURE 16.1.6 Polarization ellipse.

$$E = C[x(r_a \cos\phi + j\sin\phi) + y(r_a \sin\phi - j\cos\phi)]\exp(-jkz)$$

When the z-phase dependence is neglected except for the sign, the normalized fields of two different plane-polarized waves with the wave number 2 propagating in the negative z direction (two antennas pointing at one another) are given by

$$E_1 = E_{1p1} = E_1 \frac{x(r_1 \cos\phi_1 + j\sin\phi_1) + y(r_1 \sin\phi_1 - j\cos\phi_1)}{\sqrt{r_1^2 + 1}} \tag{30}$$

$$E_2 = E_{2p2} = E_2 \frac{x(r_2 \cos\phi_2 + j\sin\phi_2) + y(r_2 \sin\phi_2 + j\cos\phi_2)}{\sqrt{r_2^2 + 1}} \tag{31}$$

A chart of polarization loss between two elliptically polarized waves with arbitrary axial ratio is given in Fig. 16.1.7. Table 16.1.1 enables the calculation of polarization loss between plane-polarized waves for three different configurations, and for the general case.

Radiation Impedance

The complex Poynting vector $P = \mathbf{E} \times \mathbf{H}^*$ can be integrated over a closed surface about an antenna to give

$$\int\int_{s'} \mathbf{E} \times \mathbf{H}^* \cdot ds = 4j\omega(\mathrm{W}_m - \mathrm{W}_f) + \mathbf{P}_s = \mathbf{V}\mathbf{I}^* \tag{32}$$

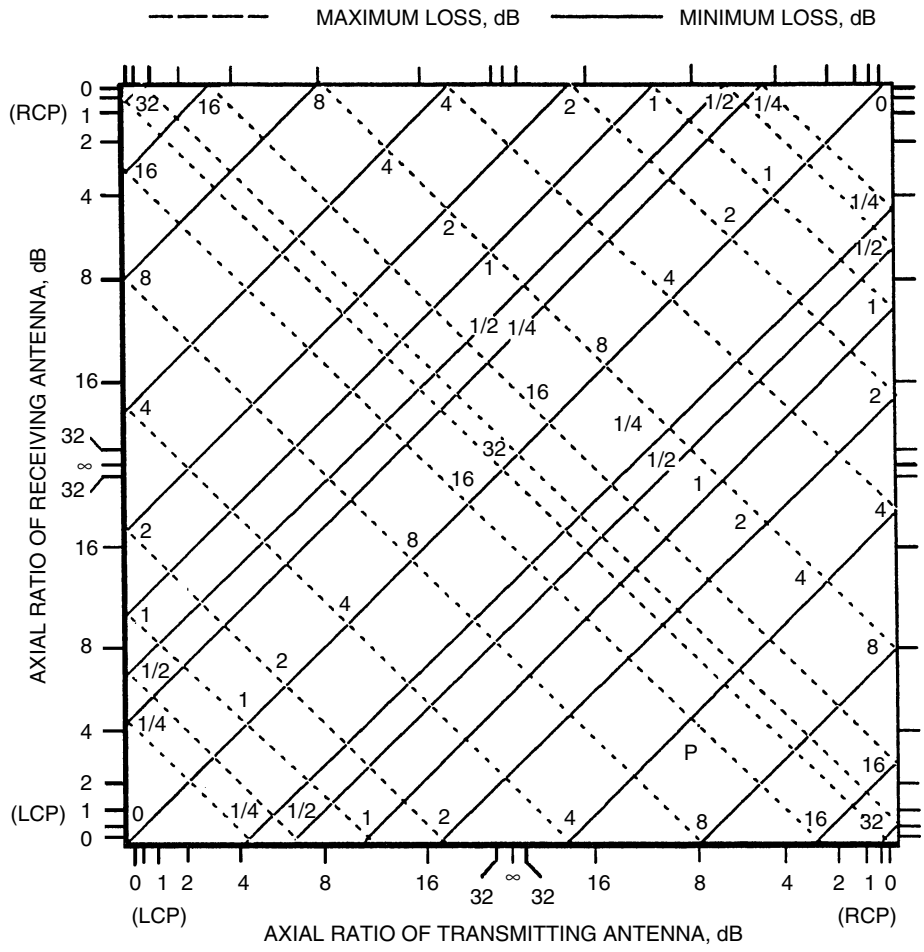

FIGURE 16.1.7 Polarization loss between two elliptically polarized wares.

Where $W_m - W_f$ = time-average net reactive power stored within the volume enclosed by S' and P_s = net real power flow through S'. As a result, the real power can be related to a radiation resistance and the reactive power to a radiation reactance by equating this total complex power to an equivalent voltage V and current I at a defined set of terminals. This radiation impedance, which is a lumped-circuit-element description of an antenna, is defined at a specific set of terminals or terminal plane which may be the aperture of a waveguide antenna. The simplest term to determine in Eq. (32) is the radiated power P_s and the corresponding radiation resistance Rr. This is true because the surface S' may be chosen in the far field of the antenna, where fields with only $1/r$ dependence are important. The radiation reactance is determined by choosing S' close to the antenna and integrating fields where $1/r^2$ and $1/r^3$ terms are important. A convenient surface to choose for these calculations is a sphere of radius r surrounding the antenna.

TABLE 16.1.1 Polarization Loss Between Plane-Polarized Waves

Type	ρ_1	ρ_2	$\lvert\rho_1 \cdot \rho_2\rvert^2$
Linear to linear $r_1 = r_2 \to \infty$	$x\cos\phi_1 + y\sin\phi_1$	$x\cos\phi_2 + y\sin\phi_2$	$\cos^2(\phi_1 - \phi_2)$
Linear to circular ($r_1 = 1$, $\phi = 0$ to π)	$\dfrac{x \pm jy}{\sqrt{2}}$	$x\cos\phi_2 + y\sin\phi_2$	$\dfrac{1}{2}$
Circular to circular	$\dfrac{x+jy}{\sqrt{2}}$	$\dfrac{x+jy}{\sqrt{2}}$	1
$r_1 = r_2 = 1$ $\phi_1 = 0$ or η $\phi_1 = 0$ or η	$\dfrac{x+jy}{\sqrt{2}}$	$\dfrac{x+jy}{\sqrt{2}}$	0
General case	$\dfrac{x(r_1\cos\phi_1 + j\sin\phi_1)}{\sqrt{r_1^2+1}} + \dfrac{y(r_1\sin\phi_1 + j\sin\phi_1)}{\sqrt{r_1^2+1}}$	$\dfrac{x(r_2\cos\phi_2 - j\sin\phi_2)}{\sqrt{r_1^2+1}} + \dfrac{y(r_2\cos\phi_2 + j\cos\phi_2)}{\sqrt{r_1^2+1}}$	$\dfrac{(1+r_1^2+r_2^2+r_1^2r_2^2+4r_1r_2)+(1+r_1^2r_2^2-r_1^2-r_2^2)\cos^2(\phi_1-\phi_2)}{2(r_1^2+1)(r_2^2+1)}$

PROPERTIES OF ANTENNAS AND ARRAYS

Radiation Resistance of Short Current Filament

The far fields of a current filament from Eq. (3) are

$$E_\theta = \frac{jkI_0\eta L \sin\theta \exp(-jkr)}{4\pi r} \qquad H_\phi = \frac{jkI_0 L \sin\theta \exp(-jkr)}{4\pi r} \tag{33}$$

When these fields are used, P_s from Eq. (33) is given by

$$P_s = \int_0^{2\pi}\int_0^{\pi} E_\theta H_\phi^* \sin\theta r^2 \, d\theta \, d\phi = \frac{\eta\pi I_0^2}{3}\left(\frac{L}{\lambda}\right) = I_0^2 R_r \tag{34}$$

Array Impedance

The pattern expressions given earlier for arrays have neglected coupling between elements in the array. Mutual coupling will not only affect the input impedance of each element input terminal as a function of scan angle but will also change the pattern of each element in a manner dependent on the element location in the array. The determination of the mutual and self-impedance of an element in an array and the effect of these changes on array patterns is a specialized problem. In general, however, arrays of antennas radiating into a linear medium will have to satisfy the same equations as any linear system with n pairs of terminals, or

$$V_1 = Z_{11}I_1 + Z_{12}I_2 + \cdots + Z_{in}I_n V_n = Z_{n1}I_1 + Z_{n2}I_2 + \cdots + Z_{nn}I_n \tag{35}$$

Input Impedance as a Function of Scan Angle

As a first approximation a large array can be treated as large continuous aperture. Wheeler[9] has shown that the impedance of a large aperture approximation in an array may be thought of as an impedance sheet whose normalized impedance and reflection coefficient vary as

$$\eta_{aperture} = (1 - \sin^2\theta \cos^2\phi)/\cos\theta \tag{36}$$

which results in

$$|\Gamma| = \tan^2(\theta/2) \tag{37}$$

for $\phi = 0°$ or $\pi/2$. This simple impedance-sheet concept acts as an upper bound on the input-impedance variation of the central element of a large array as a function of scan angle. Perhaps this model inspired the erroneous description of the scan-angle reflection peak as related to a surface wave for uncoated arrays. An indication of the accuracy of this simple bound is given in Fig. 16.1.8 from dipole calculations by Allen.[10] It should be noted that the reflection peak is the result of a null in the element pattern of each element in the infinite array at the scan angle corresponding to the reflection peak. For waveguide arrays the addition of fences in between waveguides will extend the scan-angle range to wider angles by filling in the reflection null in the element patterns. The impedance variation as a function of scan angle, for infinite arrays, can be obtained using waveguide simulators.[11,12]

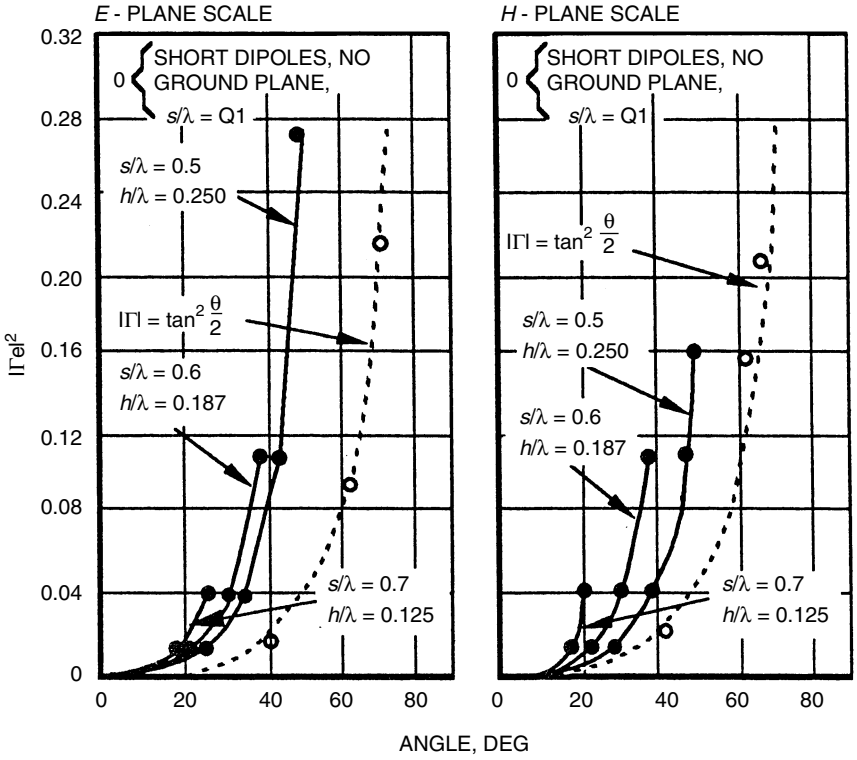

FIGURE 16.1.8 Reflection coefficient as a function of scan angle.[10]

REFERENCES

1. Croswell, W. F., and C. R. Cockrell, "An omnidirectional microwave antenna for use on spacecraft," *IEEE Trans. Antennas Propag.*, July 1969, Vol. AP-17, pp. 459–466.
2. Wong, J. L., and H. E. King, "Directivity of a uniformly excited M × N array of directive elements," *IEEE Trans. Antennas Propag.*, May 1975, Vol. AP-23, pp. 401–405.
3. H. E. King, et al., "Directivity of a Uniformly Excited N × N Array of Directive Elements," The Aerospace Corp., Aerospace TR-0074 46241-1, November 21, 1973.
4. Milligan, T. A., "Modern Antenna Design," McGraw-Hill, 1985, p. 177.
5. Sciambi, A. F., "The effect of the aperture illumination on the circular aperture antenna pattern characteristics," *Microwave J.*, August, 1965, pp. 79–84.
6. Otoshi, T. Y., "The effects of mismatched components on microwave noise-temperature calibrations," *IEEE Trans. Microwave Theory Tech.*, September 1968, Vol. MTT-16, No. 9, pp. 675–687.
7. Hollis, J. S., et al., "Microwave Antenna Measurements," *Scientific Atlanta*, 1970.
8. Offutt, W. B., and L. K. DeSize, "Methods of Polarization Synthesis, Chapter 23, Antenna Engineering Handbook," McGraw-Hill, 1993, pp. 23–29.
9. Wheeler, H. A., "Simple relations derived from a phased-array made of an infinite current sheet," *IEEE Trans. Antennas Propag.*, July 1965, Vol. AP-13, pp. 506–514.

10. Allen, J. L., "On array element impedance variation with spacing," *IEEE Trans. Antennas Propag.*, May 1964, Vol. AP-12, p. 371.
11. Hannan, P. W., and M. A. Balfour, "Simulation of a phased array antenna in a waveguide," *IEEE Trans. Antennas Propag.*, May 1965, Vol. AP-13, pp. 342–353.
12. Balfour, M. A., "Phased array simulators in waveguide for a triangular array of elements," *IEEE Trans. Antennas Propag.*, May 1965, Vol. AP-13, pp. 475–476.